POLITECNICO
MILANO 1863

SCUOLA DI INGEGNERIA INDUSTRIALE
E DELL'INFORMAZIONE

EXECUTIVE SUMMARY OF THE THESIS

Inertia Supervision for BESS Grid-forming Inverter

TESI MAGISTRALE IN Electrical ENGINEERING – INGEGNERIA Elettrica

AUTHOR: Seifeldin Nafea

ADVISOR: Roberto Perini

Co-advisor: Francesco Palombi

ACADEMIC YEAR: 2023-2024

1. Introduction

The continuous rise of renewable energy generation has led to the increase of power converters, interfacing with the grid. Moreover, this rise is causing a reduction in the traditional sources, synchronous generators, leading to an overall decline in the units supporting the grid and the system inertia.

As a result, the control family, known as grid-forming inverters, is becoming more familiar, allowing the inverters to mimic the behavior of a synchronous machine, providing its functionalities such as primary frequency control, oscillation damping, and contributing to system inertia.

Grid-forming inverters work basically by controlling the voltage magnitude and angle at the point of connection of the inverter. A major drawback of such implementation is that the current can reach high values and damage the inverter. To solve this issue, Cascaded controllers are used to limit the current [1]

Grid-forming inverters can be classified according to two main categories: Droop Control and Virtual Synchronous Generator [2]. Under each category, there exists multiple control methods.

The droop control lacks inertia. However, by adding a filter to the power measurement, an emulation with the swing equation exists for the droop, allowing it to provide inertia. However, tuning the dynamic response in that case is difficult due to the correlation between inertial and dynamic behavior.

The virtual synchronous generator category models the inverter to behave as a synchronous machine. Depending on the control method, the inverter can emulate the full dynamic model of the synchronous generator like in The VISMA control

model [2]. On the other hand, Synchronverter represents the dynamics of generator from the grid point of view [2]. However, both control structures cannot limit the current directly from the control loop, by using cascaded controllers, instead the current is limited from the physical system or by using another control block that overrides the signals from these grid-forming control methods.

A simpler control topology is suggested by [1], called Virtual Synchronous Machine (VSM), that emulates the swing equation of the synchronous machine, capturing the main two aspects of generator, inertia and damping properties, removing further complexity of the full dynamic model, and allowing the implementation of cascaded controllers.
The Thesis objective is to choose the most suitable grid-forming technology for inertia supervision applications. According to the information gathered from the literature, The VSM is chosen for detailed analysis.

2. Design of Controllers

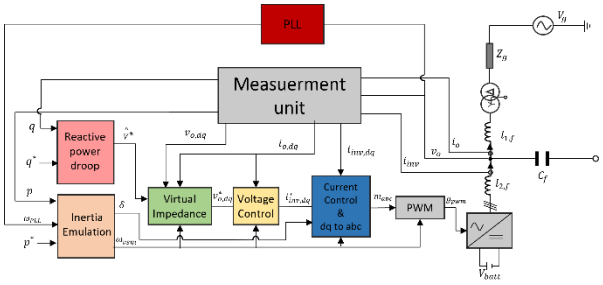

Figure 1. General Control Structure of Inverter

The Complete control structure implemented is presented in Figure 1. This structure is applied on a physical system represented in Figure 2. The parameters of the physical system are summarized in Table 1.

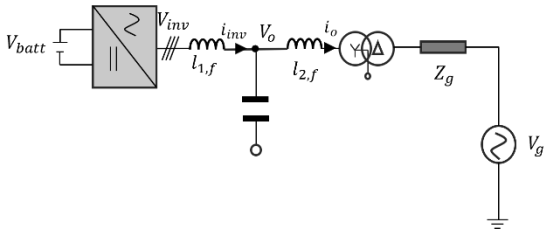

Figure 2. Physical system schematic.

A virtual impedance is used to decouple the active and reactive power flows. The virtual impedance is selected to have a 0.2 per unit inductance with zero resistance. This value ensures a high X/R ratio for the transmission line and a power-angle transient stability.
The outer voltage controller removes steady-state errors in following voltage references and provide the input signal for the current controller. The current controller aims to control the current, especially when saturation is needed for the current to avoid exceeding the inverter ratings.
A Phase locked loop (PLL) is used to measure the grid frequency at the capacitor node to be implemented in the inertia emulation block (Fig.1). It removes the codependence between inertial and dynamic response, thus improving the transient behavior.
The reactive power droop aims to regulate the voltage at the point of connection by using a droop. The value of droop, found in Table 2, depends on the inverter rating and maximum allowable voltage variation.

Table 1. Values of Physical system Parameters

Parameters	Values	Parameters	Values
V_{batt}	1300 [V]	$R_{1,f}$	0.0031 [ohm]
frequency	50 [Hz]	$R_{2,f}$	$13*10^{-6}$ [ohm]
V_g	15 [kV]	C_f	$96*10^{-5}$ [F]
R_g	0.0356 [ohm]	V_{inv} rated	690 [V]
L_g	1.119 [H]	Rated Power	1 [MVA]
$L_{1,f}$	10^{-3} [H]	X_T (Transformer)	0.06 [pu]
$L_{2,f}$	$4*10^{-6}$ [H]	R_T	0.003[pu]
SCR	10		

Current Controller

The closed loop block diagram of the current controller is shown in Figure 3 in per unit [3].

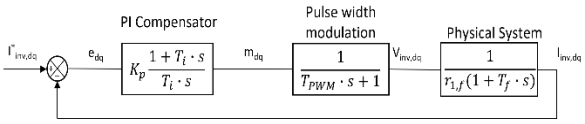

Figure 3. Closed loop block diagram of current controller

The transfer function of the pulse width modulation can be neglected if the bandwidth of the current controller is 10 times smaller than the bandwidth of the PWM. The PWM transfer function is neglected in the design process and the open loop transfer function is obtained in (1).

$$H_{OL} = \frac{K_{p,c}\left(1 + T_{i,c} \cdot s\right)}{r_{1,f} \cdot T_{i,c} \cdot s\left(1 + T_{f,c} \cdot s\right)} \qquad (1)$$

Where,

$$T_{i,c} = \frac{K_{p,c}}{K_{i,c}} \qquad , T_{f,c} = \frac{l_{1,f}}{\omega_b \cdot r_{1,f}} \qquad (2)$$

ω_b is the base angular frequency, $l_{1,f}$ is the filter inductance, $r_{1,f}$ is the filter resistance, and $K_{p,c}$ and $K_{i,c}$ are the proportional and integral gains respectively. The tuning of PI controller is based on

modulus optimum criterion [1]. The zero of the controller is canceled out with the pole of physical system. Then, the time constant of the current controller (T_c) is selected to have a bandwidth smaller than PWM but high enough to allow the voltage controller to have a relatively high bandwidth to prevent interference with the inertia emulation block. The resulting controller parameters are given by (3)

$$K_{p,c} = \frac{l_{1,f}}{T_c \cdot \omega_b} \quad , K_{i,c} = \frac{r_{1,f}}{T_c} \qquad (3)$$

The time constant chosen for the current controller is around 0.2 ms.

Voltage Controller

The closed loop block diagram of the voltage controller is shown in Figure 4 in per unit.

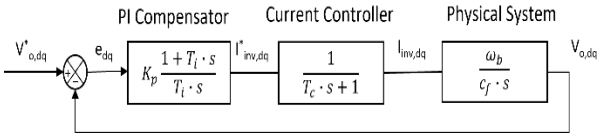

Figure 4. Closed loop block diagram of voltage controller.

The open loop transfer function is defined by (4), refereeing to Figure 4 [1].

$$H_{OL} = \frac{K_{p,v}\left(1 + T_{i,v} \cdot s\right) \cdot \omega_b}{T_{i,v} \cdot s\,(1 + T_c \cdot s) \cdot c_f \cdot s} \qquad (4)$$

c_f is the filter capacitor, while T_c is the current controller time constant. The PI controller is tuned according to symmetrical optimum criterion to obtain the maximum phase margin at the cut-off frequency [1]. The resulting controller parameters are expressed in terms of a design parameter 'a', as defined in (5), that relates tuning of the controller to the damping factor ζ.

$$K_{p,v} = \frac{c_f}{\omega_b \cdot a \cdot T_c}, \qquad K_{i,v} = \frac{K_{p,v}}{a^2 \cdot T_c} \qquad (5)$$

$$a = 2\zeta + 1$$

The design parameter value is selected to be 4 to allow the voltage controller to have a high bandwidth with a relatively low overshoot.

Phase Locked Loop

The control mechanism of the PLL is designed to regulate $V_{o,q}$(quadrature component of capacitor voltage). A filter is added to remove the measurement harmonics. Thus, the block diagram of the PLL can be defined as in figure 5 in per unit [3].

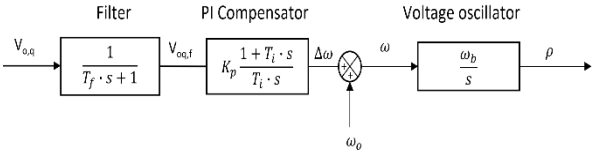

Figure 5. PLL block diagram.

The open loop transfer function is defined by (6).

$$H_{OL} = \frac{K_{p,PLL}\left(1 + T_{i,PLL} \cdot s\right) \cdot \omega_b}{T_{i,PLL} \cdot s\left(1 + T_{f,PLL} \cdot s\right) \cdot s} \qquad (6)$$

The transfer function of PLL is similar to the voltage controller. Hence, the symmetrical optimum criterion [3] will be also used to tune the PLL controller to give the following controller parameters in terms of the design parameter 'a'.

$$K_{p,PLL} = \frac{1}{\omega_b \cdot a \cdot T_{f,PLL}}, \qquad K_{i,PLL} = \frac{K_{p,PLL}}{a^2 \cdot T_{f,PLL}} \qquad (7)$$

The design parameter is chosen to get a critical damping (ζ=0.7) for the PLL.

Table 2. Values of Controllers Parameters.

Parameters	Values	Parameters	Values
$K_{p,c}$	25.2 [pu]	$K_{p,v}$	0.643 [pu]
$K_{i,c}$	79.18 [pu]	$K_{i,v}$	241.03 [pu]
T_c	0.2 [ms]	$K_{p,PLL}$	0.791 [pu]
Virtual Inductance	0.2 [pu]	$K_{i,PLL}$	81.44 [pu]
Virtual Impedance	0	$T_{f,PLL}$	1.667 [ms]
Reactive droop	0.1 [pu]		

The values of the tuned controllers are summarized in Table 2

3. Tuning of Power Block

Virtual Synchronous Machine

The VSM models an inverter to behave according to the swing equation of a synchronous generator. The swing equation is expressed in (8), in per unit.

$$T_a \frac{d\omega_{vsm}}{dt} = p_o - p_e - K_d(\omega_{vsm} - \omega_g) \quad (8)$$

T_a is the time constant, ω_{vsm} is the VSM virtual angular frequency, p_o is the power setpoint, p_e is the electric power measured, ω_g is the grid frequency and K_d is the drag coefficient. Using (8) as well as power-angle equation, the closed loop block diagram of active power is obtained in Figure 6 [4].

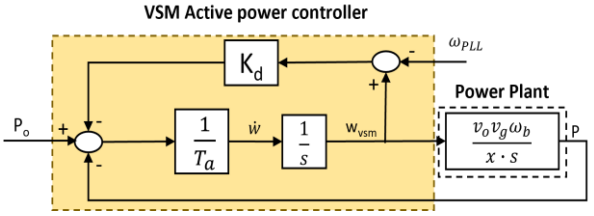

Figure 6. Closed loop block diagram of VSM power block

The closed loop transfer function is obtained from Figure 6 according to (9)

$$G_{cl,vsm}(s) = \frac{\frac{k_g}{T_a}}{s^2 + \frac{k_d}{T_a}s + \frac{k_g}{T_a}} \quad (9)$$

where

$$k_g = \frac{v_o \cdot v_g \cdot \omega_b}{x}$$

The damping ratio is calculated from (9) as shown in (10)

$$\zeta = \sqrt{\frac{k_d^2}{4 \cdot T_a \cdot k_g}} \quad (10)$$

The time constant is tuned to achieve the required inertial response. The inertial response is defined to have a power change equivalent to 0.125 per unit for every ROCOF of 1 Hz/s. By substituting these values in (11), the time constant is 6.25 s.

$$\Delta p = T_a \frac{d\omega}{dt} \quad (11)$$

The drag coefficient is then tuned to achieve a good dynamic behavior. The objective is to tune the drag coefficient to get a maximum overshoot of 10% across any short circuit value (SCR) during power setpoint changes.

The SCR is directly proportional to K_g, thus the maximum SCR is chosen for the tuning. By using (10), the drag coefficient can be tuned to obtain the minimum value of drag coefficient that corresponds to 10% overshoot.

An Important notice is that in reality, the tuning of drag coefficient is not really efficient since change in power setpoint stimulates a change in the angle of the inverter terminal, meaning that the PLL dynamics will be present. Hence, the value of minimum drag coefficient obtained from the tuning will be considered as a starting point to experimentally tune the drag coefficient in Simulink model. The drag coefficient is calculated at a value of 300 pu.

Generalized Virtual Synchronous Generator

GVSG is a control method, developed from the VSM by adding extra zero and pole in the active power block path, as shown by figure 7, to improve the dynamic behavior without using a PLL.

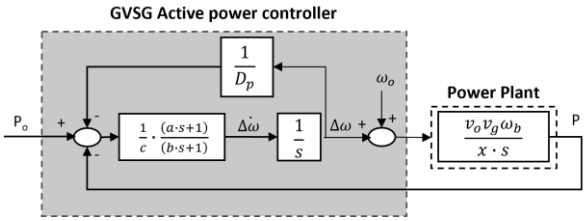

Figure 7. Closed loop diagram of GVSG power block.

It can be noticed that the drag coefficient in this control method is presented by D_p, which is the active power droop coefficient since a constant reference frequency is used. There is no PLL in this method.

The closed loop transfer function of the GVSG is written in (12) [4].

$$G_{cl} = \frac{K_g D_p (as + 1)}{D_p bcs^3 + (a + D_p c)s^2 + (1 + K_g D_p a)\, s + K_g D_p} \quad (12)$$

For the GVSG, the inertial response is tuned to be similar to VSM, thus the variable time constant of VSM and variable c of GVSG are the same as both a and b coefficients do not participate in the inertial response at steady-state.

The tuning of variables a and b is performed to achieve a good transient response through defining a set of inequality constraints.

The first constraint is concerning the Routh-Hurwitz stability criterion that can be applied to (12) to get the inequality constraint in (13) [5].

$$\begin{cases} 1 + K_g D_p a > 0 \ , & a + D_p c > 0 \\ D_p bc > 0 \\ (a + D_p c) \cdot (1 + K_g D_p a) > K_g \cdot D_p \end{cases} \quad (13)$$

The discriminant of the denominator in (12) can be represented by Δ. This third order polynomial can be seen as a second order polynomial multiplied by a first order one. To achieve a fast response, the second order polynomial should be under damped, implying the second constraint [5].

$$\Delta < 0 \quad (14)$$

The damping ratio of the under-damped system should not be smaller than the critical damping ratio [5].

$$\zeta > \zeta_{crit} \quad (15)$$

Finally, to make sure that the second order dynamics are more dominant than the first order dynamics of the third order polynomial found in the denominator of (12), the pole of the first order should be at least 5 times higher than the real value of the second order poles.

$$5\omega_n\zeta < p \quad (16)$$

The inequality constraints of (13), (14), (15), and (16) are solved using an algorithm in MATLAB to obtain a range of setpoints for coefficients a and b. Then, a setpoint is chosen randomly from this range to define variable a equal 0.126 and b equal 0.019.

Compensated Generalized Virtual Synchronous Generator

To dampen the oscillations of GVSG more. A compensator is added to the GVSG. The compensator is implemented by moving the zero of GVSG to the feedback path of the electric power. The block diagram of CGVSG is shown in Figure 8.

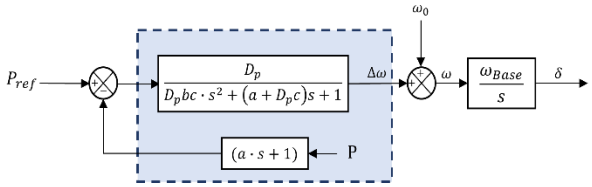

Figure 8. CGVSG power block diagram.

The tuned coefficients from the GVSG will also be used for the CGVSG.

4. Dynamic Simulations

The three control methodologies will be tested under power setpoint changes and frequency perturbations. For the case of VSM and GVSG, a constant reference frequency as well as an estimated one by the PLL will be implemented to compare the difference between them.

The control topologies are subjected to a power setpoint change that is equivalent to 0.75 per unit. The results concerning this test are shown in figure 9.

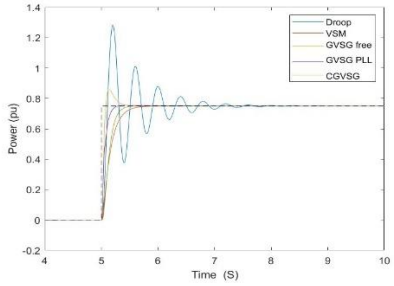

Figure 9. Inverter power after power setpoint change

The GVSG with PLL is referred to GVSG PLL, The GVSG without PLL is referred to GVSG free, and the VSM without PLL is referred to Droop.

The GVSG PLL shows the fastest response without any overshoot. Similarly, both CGVSG and VSM have no overshoot but characterized by a slower response. Both GVSG and VSM without a PLL have high dynamics and exceed the desired 10% overshoot.

A step frequency perturbation for the grid frequency is tested to check the synchronization and inertial response of these topologies. The results are shown in Figure 10.

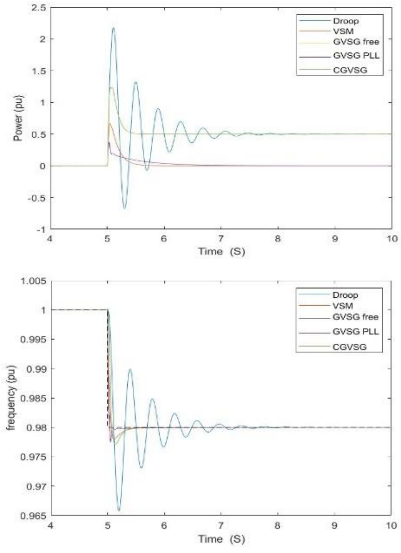

Figure 10. The top figure describes the inverter power after a step frequency, while the bottom figure shows the virtual frequency after a step frequency.

Both CGVSG and GVSG (without PLL) are showing the same inertial response, participating

with a high amount of power during frequency perturbation. The main reason is mainly due to the implementation of the droop that adds to the power change. In this simulation, the power setpoint is set to zero, and it can be noticed that technologies having the droop settle at 0.5 per unit because of the droop characteristics. Hence, the inertial response of VSM, GVSG free, and CGVSG are almost similar. However, the GVSG PLL in this case shows a low inertial participation, which is quite odd since it was characterized by the fastest response during the power setpoint test.

Finally, a ROCOF event is applied to check validity of the inertial response tuning. The results are shown in Figure 11.

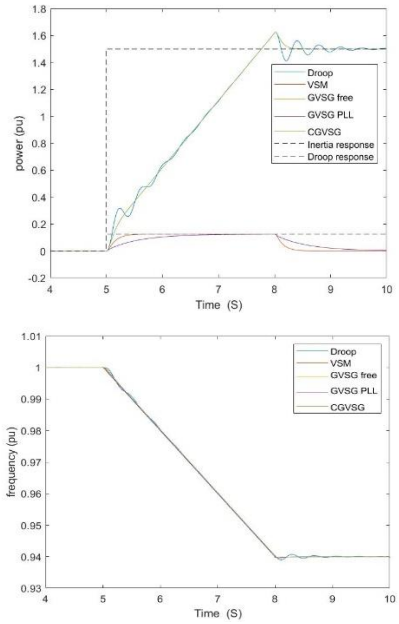

Figure 11. The top figure describes the inverter power after a ROCOF event, while the bottom figure shows the virtual frequency after a ROCOF event.

Both VSM and GVSG PLL reach the inertial power required, 0.125 per unit, according to the tuning standards. Similarly, CGVSG and GVSG free give the required inertial power, but it is integrated with the droop response. The GVSG PLL is also characterized by a very slow response in that case, which shows that it reacts very slowly to frequency perturbations.

5. Conclusions

The VSM, GVSG, and CGVSG control methodologies are the most attractive for inertial supervision based on literature findings. These controllers were tuned and tested through a dynamic model in Simulink by applying frequency and power setpoint perturbations.

The VSM and CGVSG showed the best results during the tests by having a good dynamic behavior characterized by a fast response and no overshoot, providing the required inertial power according to requirements, supporting the grid with a high inertial power during frequency perturbations.

The CGVSG is characterized by a small improvement in the response speed. However, the droop response is integrated with the inertial response, which endangers exceeding the inverter power ratings more.

A small-signal model is needed to understand the behavior of GVSG PLL and to better tune the GVSG and CGVSG according to the defined range of setpoints from solving the inequality constraints.

References

[1] S. D'Arco, J. A. Suul and O. B. Fosso, "Control System Tuning and Stability Analysis of Virtual Synchronous Machines," in IEEE Energy Conversion Congress and Exposition; Denver, CO, USA, 2013.

[2] D. B. Rathnayake, M. Akrami, C. Phurailatpam, S. P. Me, S. Hadavi, G. Jayasinghe, S. Zabihi and A. B. Bahrani, "Grid Forming Inverter Modeling, Control, and Applications," IEEE Access, vol. 9, pp. 114781-114807, 2021.

[3] F. Palombi, "HVDC INERTIA SUPPORT," Politecnico di Milano, 2018.

[4] D. B. Rathnayake, R. Razzaghi and B. Bahrani, "Generalized Virtual Synchronous Generator Control Design for Renewable Power Systems," IEEE Transactions on Sustainable Energy, vol.13, no.2, pp. 1021-1036, 2022.

[5] R. Liu, C. Xue and Y. Li, "Parameter Feasible Region Construction of Generalized Virtual Synchronous Generators with Improved Damping Capability," in 2023 11th International Conference on Power Electronics and ECCE Asia, Jeju, Korea, 2023.

6. Acknowledgement

This work is done in collaboration with NHOA Energy Company.